第 29 卷 第 6 期
2008 年 6 月
焊 接 学 报
TRANSACTIONS OF THE CHINA WELDING INSTITUTION
Vol. 29 No. 6
June 2008

电站锅炉用 HR3C 新型奥氏体耐热钢的激光焊接

吴世凯[1]， 杨武雄[1]， 肖荣诗[1]， 亓安芳[2]， 李忠杰[2]
(1. 北京工业大学 激光工程研究院，北京 100124；2. 上海锅炉厂有限公司，上海 200245)

摘 要：超(超)临界电站锅炉用新型铁素体、奥氏体耐热钢对传统焊接技术提出了挑战。激光焊接技术作为一种可靠高效的先进焊接方法，为此类钢的焊接提供了经济可行的解决办法。采用窄间隙激光填丝焊接技术，研究了10 mm厚 HR3C 新型奥氏体耐热钢管的激光焊接性，并对接头显微组织及高温持久强度进行了分析。试验采用 3 500 W Slab CO_2 激光器，填充焊丝为 T-HR3C。结果表明，通过优化激光焊接工艺参数，可以获得 X 射线探伤和渗透检验合格的焊接接头；焊缝具有明显的沿中心对称形态，以细小的柱状晶为主，混夹着少量细小的等轴晶；热影响区晶粒没有明显长大，焊缝与母材的显微硬度相当，没有明显的软化区；焊态下的激光焊接接头高温持久强度较固溶处理的热丝 TIG焊接头有明显提高。

关键词：激光焊接；电站锅炉；HR3C 奥氏体耐热钢；显微组织；高温持久强度
中图分类号：TG456.7 文献标识码：A 文章编号：0253-360X(2008)06-0093-04

吴世凯

0 序 言

为缓解全球能源紧张及环境污染问题，发展洁净煤发电技术是未来的发展趋势。而国内的一次能源结构决定以燃煤发电为主，在众多的洁净煤发电技术中最现实可行的途径就是发展超(超)临界发电技术，通过提高蒸气温度和压力，机组的热效率可大幅度地提高，供电煤耗大幅度下降。面对高的蒸气温度和压力，传统的耐热钢已不能满足使用要求，目前世界先进国家普遍采用的是新型细晶强韧化铁素体耐热钢(T23，T24，T91/P91，T92/P92，T122/P122 和 E911)和新型奥氏体耐热钢(Super304H，TP347HFG 和 HR3C)[1,2]。

目前，针对这些钢种的焊接主要采用埋弧自动焊、全位置自动 TIG 焊、混合气体半自动焊、热丝 TIG焊、瞬间液相扩散焊等方法[1,3]。这些钢种焊接时，其焊缝金属及热影响区(HAZ)性能严重劣化及奥氏体/铁素体型异种钢接头的早期失效等问题对传统焊接技术提出了挑战[4]。这是由于焊缝金属没有控轧和形变热处理的机会，晶粒不可能由此获得细化，同时供货状态优良的母材受到焊接热循环影响，接头性能劣化难以克服。研究结果表明，这种劣化的程度随焊接热输入的增大而加剧[1]。激光焊接具有能量密度高、焊接速度快、热输入小、焊接热影响区小、焊缝晶粒细小、接头强度好等优点[5]，为此类钢常规焊接时存在的焊缝韧性劣化倾向及 HAZ 蠕变强度下降等问题提供了经济可行的解决办法。

HR3C(TP310NbN)是 TP310(25 20)耐热钢的改良钢种，通过添加元素 Nb 和 N，利用弥散析出微细的金属间化合物 NbCrN 和 Nb 中的碳、氮化合物以及 $M_{23}C_6$ 碳化物进行强化。这种钢的综合力学性能优良，是蒸气温度为 620 ℃的超(超)临界锅炉过热器和再热器的首选材料[1,4]。作者采用了窄间隙激光填丝焊接技术，通过工艺参数优化，完成了 HR3C 奥氏体耐热钢管的激光焊接工艺试验。研究了激光焊接接头的组织和性能，并对比了激光焊接接头与热丝 TIG焊接头在 650 ℃时的高温持久强度性能。

1 试验方法

试验采用德国 Rofin-Sinar 公司 DC035 Slab CO_2 激光器，最大输出功率为3 500 W，光束模式为 TEM_{00} 模，焊接工作台为五轴联动工作台。光束采用抛物铜镜反射聚焦系统，焦距为 300 mm，聚焦光斑直径为0.26 mm。焊接时，装卡好的管接头在回转工作台的带动下旋转，双层喷嘴侧吹保护气。焊后用高温持久试验机进行了高温持久强度试验，用光学显微镜进行金相组织分析。

收稿日期：2007-12-17

试验用材料为日本住友金属的 HR3C 新型奥氏体耐热钢管,规格为 Φ48 mm ×10 mm。填充材料为住友金属的 T HR3C 焊丝,焊丝直径为 Φ1 mm。母材及焊丝的化学成分如表 1 所示。

表 1 母材及填充材料的化学成分(质量分数,%)

Table 1 Components of experimental materials

	C	Cr	Ni	Nb	N	Si	Mn	P	S	Cu	Mo
HR3C	≤0.10	23.0～27.0	17.0～23.0	0.20～0.60	0.15～0.35	≤1.50	≤2.00	≤0.030	≤0.030		
T HR3C	0.06	27.0	20.1	0.45	0.31	0.3	1.51	0.003	0.006	2.94	0.91

试验采用窄间隙激光填丝多层焊接技术。试验装置简图如图 1 所示。对接坡口采用 U 形坡口,其中钝边厚度为 6 mm,坡口间隙为 1.8 mm。

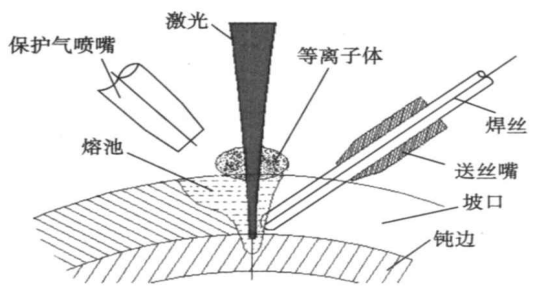

图 1 试验装置原理简图

Fig. 1 Experimental setup of laser welding

采用表 2 所示的优化工艺参数,在无焊后热处理的条件下,获得内部没有缺陷、表面成形良好的焊接接头(第一层为自熔焊接)。在 2 个试验件上取一组标准试样进行高温持久强度试验,同时取金相试样进行金相组织分析。

表 2 激光焊接工艺参数

Table 2 Laser welding parameters

	激光功率 P/W	焊接速度 v_w/(m·min^{-1})	送丝速度 v_s/(m·min^{-1})	保护气流量 q/(L·min^{-1})
第一层	3 500	1.8		2.5Ar/12.5He
第二层	3 500	0.75	3.6	5Ar/15He

2 试验结果及讨论

2.1 HR3C 的焊接性

国内对于 HR3C 奥氏体耐热钢没有使用经验,同时由于受专利保护,公开的可参考的焊接性研究几乎没有。从有限的资料来看,HR3C 焊接时的主要问题与其它奥氏体耐热钢基本相同,主要是高温裂纹、晶间腐蚀和明显的 σ 相时效析出脆化。在采用传统电弧焊接时,必须避免采用过大的热输入,并严格控制层间温度,同时冷却到马氏体转变温度以下一定时间后必须马上升温进行固溶处理[1,6]。

采用优化后的激光焊接工艺参数焊接的对接焊缝正、反面表面成形良好,经 X 射线探伤检验和渗透检验,100 %合格。解剖焊缝也没有发现气孔、裂纹等缺陷,焊缝横截面如图 2 所示。焊缝下部为自熔焊接,组织呈中心对称形态,焊缝上部具有“钉子头”形状。同时焊缝中没有观察到明显的热影响区。

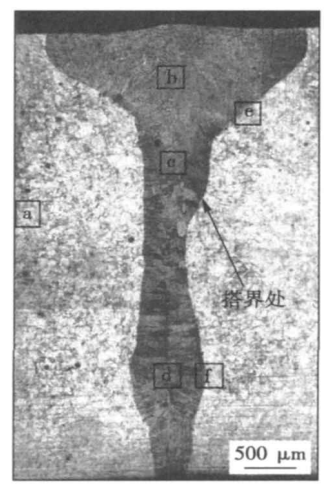

图 2 焊缝横截面

Fig. 2 Cross-section of laser welded joint

2.2 金相组织

HR3C 激光焊接接头的母材、焊缝及熔合线附近的金相组织如图 3 所示(选择区域如图 2 所示)。

分析金相组织照片可知,母材的供货状态为固溶状态,显微组织为完全奥氏体组织,并有许多孪晶出现(黑色块状物),晶粒内弥散析出微细的金属间化合物 NbCrN 和 Nb 中的碳、氮化合物以及 $M_{23}C_6$ 碳化物等强化相。受散热条件限制,焊缝中可观察到明显的沿焊缝中心对称的形态。焊缝下部组织主要为细小的柱状奥氏体组织,各晶体学取向相同的晶粒组成一个晶群,沿熔合线法线呈板条状向焊缝中

心生长,同时各板条状晶群间夹杂着细小的等轴状晶粒。而焊缝上部结晶后的组织也呈柱状向焊缝中心生长,枝晶中间夹杂着细小的等轴晶状组织,但由于填充焊丝的加入并搅拌熔池,明显的板条状晶群形态消失。在两层焊道的搭界处,沿焊缝中心对称的形态消失,为板条状奥氏体和等轴晶的混合组织。晶粒尺寸较母材大幅度减小,同时在焊缝中没有观察到δ铁素体。分析认为,搭界处焊缝的稀释率发生变化,导致该处焊缝中的合金元素局部偏析是其组织结构发生变化的原因。

尽管由于上下两层焊缝的热输入不同,但是其熔合线附近的组织基本相同,都没有观察到明显的热影响区,熔合线附近的母材晶粒也没有长大。图 4 是图 3e,f 的局部放大后的组织,可以清楚地看到熔合线约为 2 μm 的奥氏体组织。同时从图中可以看出在焊缝下部组织中,各板条状晶群从母材的奥氏体晶粒中沿不同方向向焊缝中心生长,其生长方向可能与原奥氏体晶粒的晶体学方向有关。

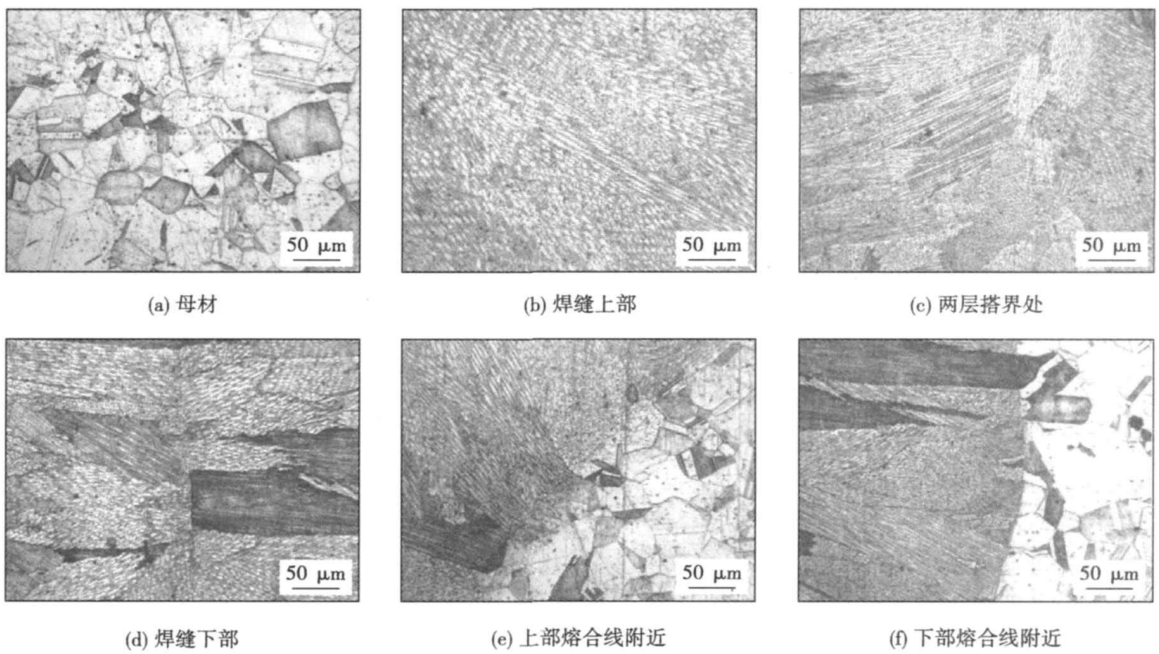

图 3　焊缝及热影响区的金相组织

Fig. 3　Microstructure of weld bead and HAZ

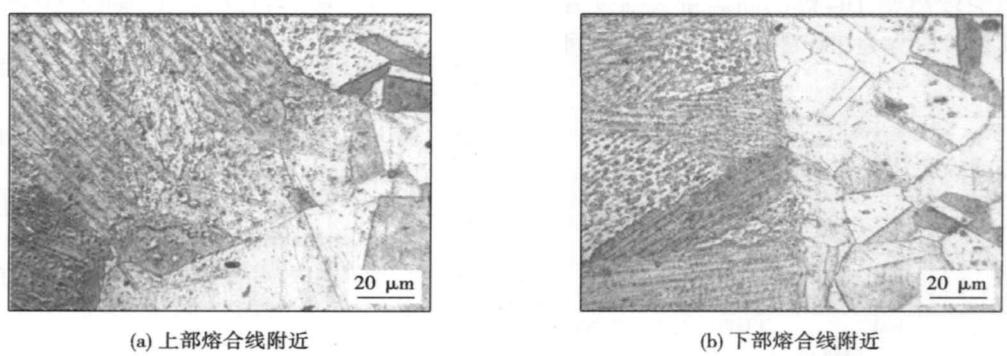

图 4　热影响区的放大组织

Fig. 4　Microstructure of weld HAZ

2.3　接头显微硬度分布

图 5 是激光焊接焊缝上部和下部的显微硬度分布曲线。从图中可以看出,焊缝与母材的硬度相当,不存在明显的软化区域,这也说明了焊缝中不存在明显的热影响区,同时不同热输入条件下的显微硬度基本相同。这是由于激光束的能量密度大,焊接

热输入小,同时由于 HR3C 的热导率较低,焊接时快的加热和冷却速度,促使热影响区变小,同时对焊接热影响区的晶粒粗化造成约束,由于基本不存在热影响区,则避免了热影响区的高温液化裂纹倾向及性能劣化。同时由于焊缝中基本为奥氏体组织,不存在淬硬组织,焊接接头也可以具有良好的韧性。

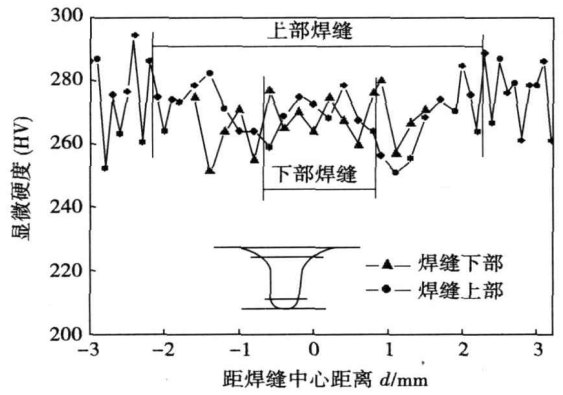

图 5 焊接接头显微硬度分布

Fig. 5 Micro-hardness distribution of laser welding joint

2.4 接头高温持久强度

由于 HR3C 主要应用于锅炉部件的高温段,其常温力学性能不是主要的评价指标,需重点考察服役条件下的高温持久强度及时效组织演变。

高温持久强度试验的试样采用标准试样,试验温度为 650 ℃。图 6 为激光填丝焊接接头与热丝 TIG 焊对接接头的高温持久强度值对比图。其中热丝 TIG 焊接头进行过焊后固溶处理。从图中可以看出,激光填丝焊较热丝 TIG 焊的高温持久强度有明显提高,尤其是在应力为 230 MPa 时,其断裂时间提高了约 160 %。其原因是由于激光焊接低的热输入和高的焊接速度,焊缝的凝固速度比较快,初次结晶的δ铁素体含量比较少,导致其高温持久强度大幅度提高。同时由于焊缝晶粒细化、非常窄的热影响区以及快速冷却抑制了初次结晶铁素体发生σ相转变也是导致持久强度提高的重要原因。

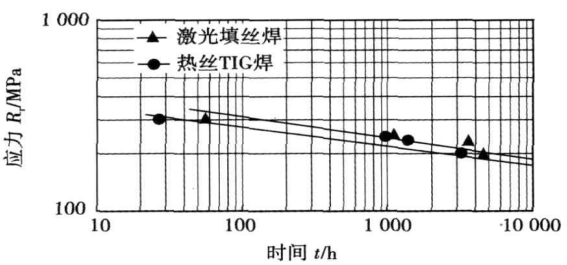

图 6 650 ℃时的高温持久强度线图

Fig. 6 High temperature lasting test at 650 ℃

3 结 论

(1) 采用激光窄间隙填丝焊接 HR3C 奥氏体耐热钢,在不采用预热和后热处理的条件下,可以获得表面成形良好,没有裂纹、气孔等缺陷的焊接接头。

(2) HR3C 激光焊接焊缝下部组织主要为细小的柱状奥氏体组织,具有明显的沿焊缝中心对称的形态;焊缝上部结晶后的组织呈柱状向焊缝中心生长,枝晶中间夹杂着细小的等轴晶状组织;在两层焊道的搭界处,沿焊缝中心对称的形态消失,为板条状奥氏体和等轴晶的混合组织。

(3) HR3C 激光焊接接头基本不存在热影响区,熔合线附近母材晶粒没有明显长大,焊缝与母材的显微硬度相当,不存在明显的软化区域。

(4) HR3C 钢激光填丝焊接接头较热丝 TIG 焊接头的高温持久强度有明显提高,即使是在没有焊后热处理的条件下也优于固溶处理的热丝 TIG 焊接头。

参考文献:

[1] 杨 富, 章应霖, 任永宁, 等. 新型耐热钢焊接[M]. 北京:中国电力出版社,2006.

[2] 杨 富, 李为民, 任永宁, 等. 超临界、超超临界锅炉用钢[J]. 电力设备,2004,5(10):41 - 46.

[3] 张贵锋, 张建勋. 日本 T91 钢管液相扩散焊技术的研究发展[J]. 电焊机,2006,36(1):37 - 40.

[4] 杨 富. 1000MW 级超超临界火电机组锅炉用新型耐热钢的焊接[J]. 中国电力, 2005, 38(8): 48 - 52.

[5] 李志远, 钱乙余, 张九海, 等. 先进连接方法[M]. 北京: 机械工业出版社,2000.

[6] 中国机械工程学会焊接学会. 焊接手册(材料的焊接)[M]. 北京: 机械工业出版社, 2001.

作者简介:吴世凯,男,1976 年出生,博士研究生。主要从事激光材料加工方面的研究工作。发表论文 5 篇。

Email: wushikai @emails.bjut.edu.cn

tensile plastic strain in the weld metal is $\Delta\varepsilon_t = (T_m - T_r) - (R_{rt} - R_{rc})/E$.

Key words: welding stress and strain; hypothesis of plain section; compressive plastic strain; tensile plastic strain

Influence of TIG dressing on fatigue property of 10Ni5CrMoV steel welded joints XUE Gang, WANG Renfu (Luoyang Ship Material Research Institute, Luoyang 471039, Henan, China). p77 - 80

Abstract: The fatigue tests were taken on the large angle welded joints of 10Ni5CrMoV steel with and without tangsten inert gas welding(TIG) dressing treatment on the toe. The fatigue life, the relation of load and stroke and the fatigue crack initiation at the same loading condition were analyzed comparatively. The welding residual stress was also measured. The stress field and the strain field of welded joints with and without TIG dressing treatment were calculated by the finite element method. The results indicate that the TIG dressing treatment can improve the fatigue property of the large angle welded joints of 10Ni5CrMoV steel. The fatigue life of the welded joints is increased 34 % by TIG dressing on the toe at the same loading condition. The primary cause is that the TIG dressing treatment can improve the weld geometry and reduce the stress concentration on the weld toe. So the stress value in the toe is reduced at the same loading condition and the fatigue ability of the welded joints is increased.

Key words: TIG dressing; 10Ni5CrMoV steel; welded joint; fatigue property

Effect of double-wire narrow gap GMA welding parametars on weld appearance ZHAO Bo, FAN Chenglei, YANG Chunli, ZHANG Liangfeng (1. State Key Laboratory of Advanced Welding Production Technology, Harbin Institute of Technology, Harbin 150001, China). p81 - 84

Abstracts: The influences of three parameters which are space between wire and edge, space between two wires and angle between two wires on weld appearance were studied in double-wire narrow gap welding with one pool by procedure experiments. The results show that the increase of space between wire and edge can make sidewall penetration and saucer shape of weld surface increase. When the arrangement of wires became parallel, sidewall penetration and saucer shape of weld surface increased to the maximum value. When space between wires increased, sidewall penetration and saucer shape of weld suface increased firstly and then decreased, and finally arrived at peak value when the space between wires is 5 - 10 mm under the co-action of arc and molten pool energy. But when there was no finger penetration, the three procedure parameters mentioned had little influence on weld penetration. There was lack of fusion of weld bottom when I-shape groove was adopted, and adjusting the three parameters could not eliminate the phenomenon of nonfusion.

Key words: narrow gap welding; twin-wire welding; weld formation

Mechanism and remedy of undercut formation during laser-arc hybrid welding GAO Ming, ZENG Xiaoyan, HU Qianwu, YAN Jun (Wuhan National Laboratory for Optoelectronics, Huazhong University of Science and Technology, Wuhan 430074, China). p85 - 88

Abstract: To enhance the reliability of laser-arc hybrid welding, undercut formation and its remedy mechanisms during this process were discussed. The results demonstrated that laser can increase undercut critical speed of hybrid welding, which reaches 5 times than that of arc welding with appropriate welding parameters. Two undercut remedying mechanism resulted from laser-arc interaction were found during hybrid welding. The one is the surface tension state of three phases (solid, liquid and gas) at weld toe is changed by laser-arc synergic effects and form a resultant force pointing to the outside of molten pool. The other is the enhancement of flow speed and time of molten metal flowing from pool center to outer by the increasing of heat input and temperature gradient in molten pool. This faster flow drives molten metal to weld toe and avoid undercut, which is the main mechanism for restraining undercut. Furthermore, the experiential formula to undercut critical speed of hybrid welding and the optimal adjusting range of arc voltage were also obtained.

Key words: laser welding; hybrid welding; undercut; critical speed

Numerical simulation of welding residual stress for longitudinal straight weld seam for aluminum alloy thin-wall cylinder ZHOU Guangtao[1], LIU Xuesong[1], YANG Jianguo[1], YAN Dejun[1], FANG Hongyuan[1,2] (1. State Key Laboratory of Advanced Welding Production Technology, Harbin Institute of Technology, Harbin 150001, China; 2. Institute of Astronautical Technology, Shenyang Institute of Aeronautical Engineer, Shenyang 110034, China). p89 - 92

Abstract: Numerical simulation of TIG welding of thin wall aluminum cylinder by thermo-elastic-plasic FEM was conducted. Based on the generation of analysis model, the values and distribution on the whole cylinder for quasi-steady temperature field and residual stress field were described quantitatively. Experiments were performed to verify the residual stress. It can be drawn that during welding there exits high temperature at the centre of heat source and its vicinity where temperature gradient keeps greater. The longitudinal residual stress in weld seam and its HAZ are tensile, its maximum is in the cross-section at the center of weld length and reached 138 MPa. The maximum compressed transverse residual stress was on the both sides of weld seam. The tensile and compressive region of longitudinal residual stress changed alternately at the circumference of cylinder. The residual stress of the welded Al cylinder has been measured by stress-release method, and excellent agreement between the measured value and calculated value is shown.

Key words: numerical simulation; temperature field; residual stress; stress measurement

Laser welding of new type austenite heat-resistant steel HR3C for ultra supercritical boilers WU Shikai[1], YANG Wuxiong[1], XIAO Rongshi[1], QI Anfang[2], LI Zhongjie[2] (1. Institute of Laser En-

gineering, Beijing University of Technology, Beijing 100124, China; 2. Shanghai Boiler Works Ltd., Shanghai 200245, China). p93 - 96

Abstract: New types of ferrite and austenite heat-resistant steels used in supercritical or ultra supercritical boilers have issued challenges to conventional welding techniques. As a reliable and advanced joining technique, laser welding may be one of the promising solutions for the welding of these steels due to the low heat input. A slab CO_2 laser with an output power of 3 500 W was applied and the narrow gap laser welding process was adopted with T - HR3C filler wire to weld HR3C tubes of the new type austenite steel with a thickness of 10 mm. The joint microstructure and high temperature lasting strength were investigated. It is found that a sound joint can be obtained by optimizing the process parameters. The microstructures in the weld bead are fine column austenite grains with a few fine equiaxed austenite grains, appear more or less symmetrically along the bead center. The grain size in the HAZ is not obviously coarsening. The micro-hardness in the weld is correspondence with that of the base metal, and no obvious softened zone is observed. The high temperature lasting strength of the laser welded joint in the as-welded condition is distinctly improved compared to that of TIG welding joint with post-weld heat treatment.

Key words: laser welding; power boiler; HR3C austenite heat-resistant steel; microstructure; high temperature lasting

Influence of welding parameters on laser-induced plasma temperature in CO_2 laser welding of aluminum alloys QI Junfeng, DING Peng, ZHANG Dongyun, ZUO Tiechuan (Institute of Laser Engineering, Beijing University of Technology, Beijing 100022, China). p97 - 100

Abstract: The spectrums of laser-induced plasma in CO_2 laser welding of 6061 aluminum alloy are measured through PI Pro2500i transient spectrometer. Boltzmann diagrams can be used to calculate the average temperature of laser-induced plasma, which are deduced from Mg Ⅰ spectrums between 200 - 600 nm. The influence of welding parameters, such as laser power, welding speed, focus position and shielding gas, on laser-induced plasma temperature are investigated separately and the reasons are also discussed. Under the experimental conditions, laser power plays little role on laser-induced plasma temperature (6 000 K) when it exceeds the threshold power of laser penetration welding. The effect rule of welding speeds on laser-induced plasma temperature likes inverted U curve. Laser-induced plasma temperature has been increased and then decreased when the flow rate of shielding gas is increased for a given diameter of nozzle. Laser-induced plasma temperature will increase 500 - 1 000 K when adding argon in to helium.

Key words: laser welding; aluminum alloys; laser-induced plasma; spectrum

Effect of welding with trailing rotating extrusion on microstructure and mechanical properties of aluminum alloy welded joints LI Jun, YANG Jianguo, WENG Lulu, FANG Hongyuan (State Key Laboratory of Advanced Welding Production Technology, Harbin Institute of Technology, Harbin 150001, China). p101 - 104

Abstract: Welding with trailing rotating extrusion (WTRE) is a new technology to improve the microstructure and mechanical properties of welded joints as well as control welding residual stresses and distortion of thin-walled structures. The metallographs of 2A12-T4 aluminum alloy welded joints show that the microstructure of the WTRE welds are more compact with refined crystal grains and less welding defects such as air cavities and shrinkage porosities than the ones of the conventional welds. The results of tensile and bending tests show that such mechanical properties as tensile strength and three-point bending strength of the welded joints are enhanced markedly. The cracks in some WTRE test pieces started from the weld center rather than the weld toes, which were strengthened by the rotating extrusion operation.

Key words: welding with trailing rotating extrusion; aluminum alloy; microstructure; mechanical properties

Effect of spherical radius of spot welding electrode on nugget size LI Rujuan, LI Mengsheng, WANG Yang, YAN Hongdan (Hefei University of Technology Academy of Material, Hefei 230009, China). p105 - 108

Abstract: Spherical radius is a very important factor which can affect the quality of spot welding. After solving the contact problem, an axial symmetry model to simulate the welding process was established. Effects of spherical radius of electrode on low-carbon steel resistance spot welding nugget size were investigated quantitatively through ANSYS software. Nugget sizes were simulated by adopting different eletrode radius, and accuracy of simulation was verified by welding experiment. Results indicate that electrode spherical radius has great effects on the nugget diameter and penatration rate, while has few effects on the size of heat-affersted zone. Results also show the error is less than 10 % between simulated value and test value.

Key words: spot welding; temperature field; numerical simulation

Microstructure and properties of aluminum coatings on Al alloy surface by arc spraying XU Rongzheng, SONG Gang, LIU Liming (State Key Laboratory of Materials Modification, Dalian University of Technology, Dalian 116024, Liaoning, China). p109 - 112

Abstract: The pure aluminum coatings on 6061 Al alloy were prepared by arc spraying. The microstructure and porosity of the coating were observed by means of optical microscope. The evaluation of the corrosion properties of the coatings was carried out through the simulated immersing tests, salt spray test and electrochemical experiment in 5 % NaCl solution. The results showed that the pure aluminum coating was homogeneous and dense, as well as lower porosity. The coatings can protect the Al alloy substrate from corrosion. The corrosion resistance of the coating with sealing was better than that of the coating without sealing.

Key words: Al alloy; aluminum coating; arc spraying; corrosion resistance